Supporting Information

The Effects of ZSM-5 Mesoporosity and Morphology on the Catalytic Fast Pyrolysis of Furan

Jinsheng Gou,[ab‡*] Zhuopeng Wang,[b‡] Chao Li,[bc] Xiaoduo Qi,[b] Vivek Vattipalli,[b] Yu-Ting Cheng,[b] George Huber,[d] William C. Conner,[b] Paul J. Dauenhauer,[e] T. J. Mountziaris[b] and Wei Fan[b*]

a. College Materials Science & Technology, Beijing Forestry University, Key Laboratory of Wooden Material Science and Application, Ministry of Education, 35 Qinghua East Road, Haidian District, Beijing, China, 100083

b. Department of Chemical Engineering, University of Massachusetts, 159 Goessman Lab, Amherst, 686 N Pleasant Street, Amherst, MA, 01003

c. School of Chemistry and Chemical Engineering, South China University of Technology, 381 Wushan Road, Tianhe District, Guangzhou, China, 510641

d. Department of Chemical and Biological Engineering, University of Wisconsin Madison, 1415 Engineering Drive, Madison, WI, 53706

e. Department of Chemical Engineering and Materials Science, University of Minnesota, 421 Washington Ave. SE, MN, 55455

‡:Equal contribution from the authors.

* Corresponding authors.

Reaction section

The furan conversion using a flow fixed bed reactor has been described in detail elsewhere[1, 2]. The catalytic fast pyrolysis reactions were carried out in a continuous flow fixed-bed quartz rector of ½ in. O.D. The reactor (Figure S1) was placed into a PID controlled furnace vertically. The temperature of the reactor was measured using a thermocouple (Omega,) which was inserted on the top of the catalyst bed. Catalyst powders were held in the middle of the reactor by a quartz frit. Prior to the reactions, the catalyst bed was calcined at 600 °C under 60 mL/min air flow for 2 hours. After calcination, the reactor and succeeded pipes were flushed by helium (Middlesex, 99.999%) at 600 °C under 408 mL/min for 5 min respectively. The helium stream then was switched to bypass the reactor. Furan was pumped into the helium stream by a syringe pump (Fisher, KDS100). The syringe used for pumping furan was Hamilton gastight syringe with customized needle length of 300 mm. Prior to the run, the helium stream, in which furan was carried, bypassed the reactor for 30 min before switching it to go through the reactor. All runs were done at atmospheric pressure. No pressure drop was detected across the catalyst bed. Gas phase products were collected by air bags (SKC, Tedlar). An air bath condenser was used to trap the heavy

products. After reaction, the reactor was flushed by helium at the reaction temperature with a flow rate of 408 mL/min for 45 s. The effluent was collected by an air bag. After reactions, the spent catalyst was calcined at 600 °C under 60 mL/min air flow for 1 hour. The CO formed during this calcination was converted to CO_2 by a copper converter (copper oxide, CuO, Sigma-Aldrich) working at 240 °C. CO_2 was then trapped by a CO_2 trap (Ascarite, Sigma- Aldrich). Coke yield was obtained by weighing the weight change of the CO_2 trap.

Condensed products were extracted by 10 mL of ethanol from the air condenser to obtain the liquid products. Both liquid and gas products were identified by GC/MS (Agilent-7890B GC coupled with 5890 MS) and quantified by GC/FID/TCD (Agilent 6890B for hydrocarbons and Agilent 7890B for CO and CO_2).

The GC-FID was calibrated by C2-C6 normal olefins standards (Scott Specialty Gas, 1000 ppm for each olefin), furan(g), benzene(g), toluene(g), xylenes(g) (which was injected as liquid phase into gas bag and vaporized at room temperature), ethylbenzene(l), styrene(l), indene(l), naphthalene(l), and benzofuran(l). The sensitivity of other hydrocarbons was assumed to be proportional to the number of carbon of molecules with similar structure (e.g. styrene vs. methylstyrenes; indene vs. methylindenes). The GC- TCD was calibrated by CO and CO_2 standards (Airgas, 5% CO_2 and 5% CO, balanced by helium).

In our study, less than 0.05% carbon or products were collected in the condenser. The majority of the products were either in the gas phase or being coke and deposited on the catalyst. Our carbon balances closed with 95% for all runs.

Standard reaction conditions for furan catalytic fast pyrolysis in the continuous flow fixed-bed reactor were 600 °C, WHSV 9.5 h^{-1}, and partial pressure 5.5 torr. Furan was pumped with a pumping rate 0.58 mL/h, and the carrier gas was controlled at 408 mL/min. The amount of catalyst that was loaded into the reactor was typically 57 mg. All the reactions were run at least 3 times and the mean data was used.

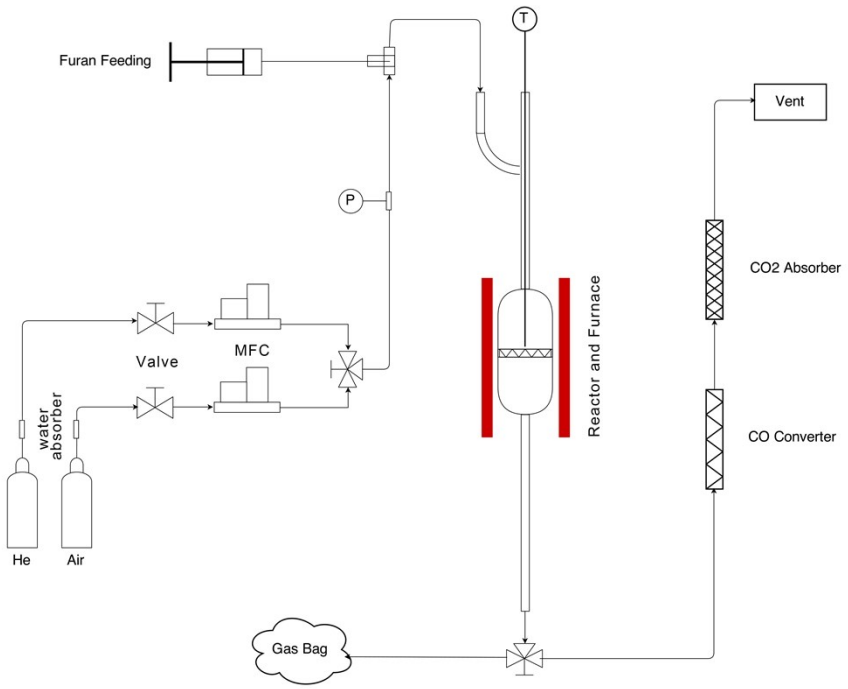

Figure S1. A continuous flow fixed bed reactor used for furan catalytic fast pyrolysis

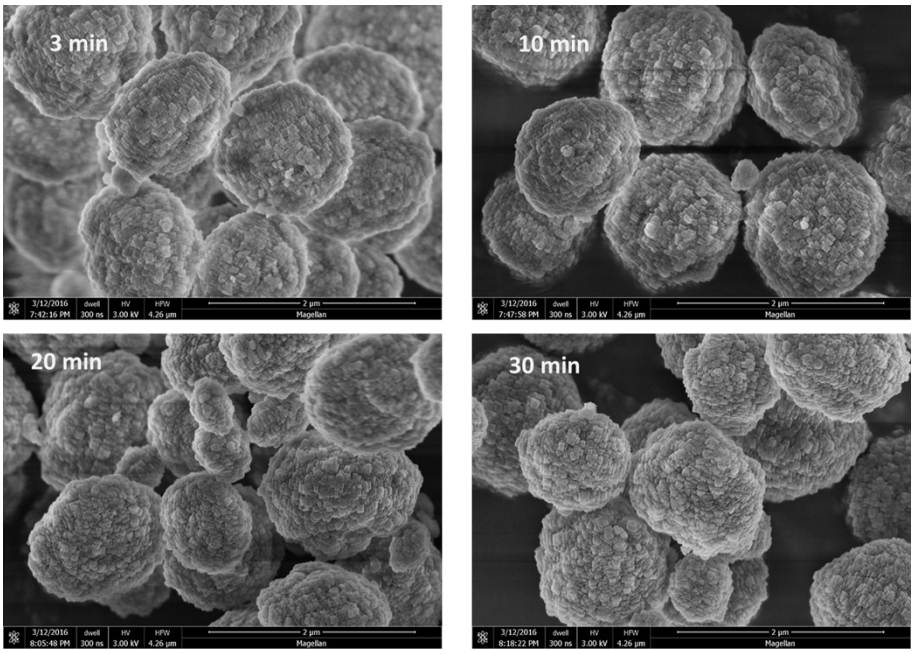

Figure S2. SEM images for meso ZSM-5 samples after CFP of Furan with the time on stream from 3 min to 30 min.

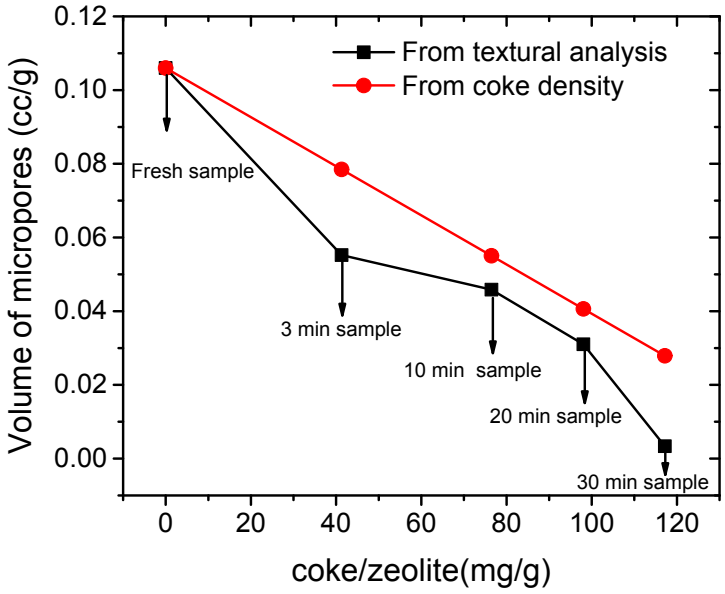

Figure S3. Correlation of micropore volume and weight of formed coke over mesoporous ZSM-5 catalyst. The density of coke used in the calculation is 1.5 g/cm^3

ZLC Model and Analysis Method

The 3D spherical ZLC model was used in this study to analyze the desorption data. The model assumes the desorption step is entirely controlled by the intra-crystalline diffusion and the surface of the zeolite is constantly at equilibrium with the bulk phase. The model can be described by[3]:

Governing equation with a spherical coordinate:

$$\frac{\partial q}{\partial t} = D\nabla_r^2 q \tag{S1}$$

The initial and boundary conditions:

$$q(r,0) = q_0 = KC_0, \quad C(0) = C_0 \tag{S2}$$

$$\frac{\partial q}{\partial r}(0,t) = 0 \tag{S3}$$

$$-D\frac{\partial q}{\partial r}(R,t) = \frac{1}{3}\frac{F\ R}{V_S K} q(R,t) \tag{S4}$$

Where q is the solid phase concentration; *D* is the micro-pore transport diffusivity; *C* is the gas phase concentration; *K* is Henry's constant; *R* is radius of zeolite particle; *F* is flow rate of purge flow; *Vs* is volume of the zeolite bed; *t* is time variable. The second boundary condition is derived from the mass balance within the entire ZLC column assuming gas phase accumulation is neglected. The solution to the boundary value problem has been solved in the literature[4]:

$$\frac{c}{c_0} = 2L\sum_{n=1}^{\infty} \frac{exp(-\frac{\beta_n^2 Dt}{R^2})}{\beta_n^2 + L(L-1)} \tag{S5}$$

Where

$$\beta_n cot\beta_n + L - 1 = 0 \tag{S6}$$

And

$$L = \frac{1}{3}\frac{F\ \ R^2}{KV_S D} = \frac{\tau_{Diffusion}}{\tau_{convenction}} \tag{S7}$$

L represents the ratio of micro-porous diffusional time constant to the external transport time. Where τ is time constant; β has no physical meaning. The desorption process is diffusion controlled if $L > 10$ and equilibrium controlled when $L < 1$[3]. At long time (*t* value is large), only the first term in Eq. S5 contributes to the summation and S5 reduces to:

$$\frac{c}{c_0} = \frac{2L}{\beta_1^2 + L(L-1)} exp(-\frac{\beta_1^2 Dt}{R^2}) \quad \text{(S8)}$$

Thus, from Eq.S8, the inverse of micro-pore diffusion time constant $\frac{D}{R^2}$ can be evaluated from the slope of the plot of $Ln\left(\frac{C}{C_0}\right)$ versus *t* at long time region. This method is called Long Time (LT) analysis.

ZLC verification

In order to interpret the ZLC data correctly, the desorption step needs to be controlled by the intra-crystalline diffusion[3]. Such a condition can be confirmed either from the value of L or from the flow study.

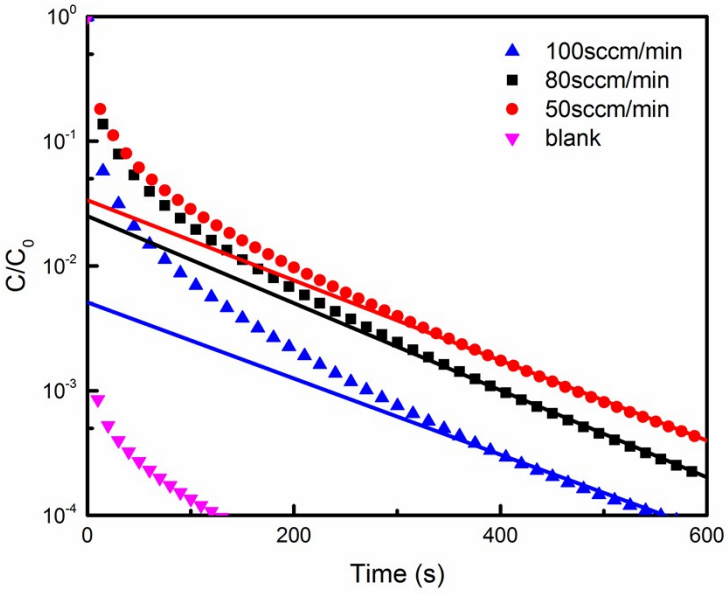

Figure S4. ZLC blank run and flow study of cyclohexane on fresh meso ZSM-5 at 130 °C under different washout flow rate.

Figure S4 shows the blank study and different flow study to validate the ZLC experiments. The blank run was carried out by loading an empty column to the system, and the delay from the desorption (around 125 s) is caused purely by the experimental set-up. As shown in the Figure, compared to the desorption curve with zeolite, the delay from the system itself is minimal (125 s compare to 375 s). Thus, the desorption curve obtained from the actual ZLC experiments (with delay greater than 130 s) were indeed controlled by the desorption process through the zeolite. The flow study was performed by changing the desorption flow rate with the same zeolite loading. It can be seen that different flow rates yield a series of parallel desorption curves, meaning that the convection flow didn't affect the D/R^2 value

extrapolated from the slope of the desorption curve, and therefore, it indicates that the overall desorption process is entirely controlled by the intra-crystalline diffusion.

Table S1. Parameters obtained from ZLC study

	Fresh Sample			3 min coked sample			30 min coked sample		
Temp. (° C)	$D/R^2(s^{-1})$	L	β	$D/R^2(s^{-1})$	L	B	$D/R^2(s^{-1})$	L	β
90	2.58×10^{-4}	267.12	3.1298	2.74×10^{-4}	362.32	3.1329	2.91×10^{-4}	1521.95	3.1395
110	4.00×10^{-4}	262.43	3.1296	3.97×10^{-4}	426.35	3.1342	3.99×10^{-4}	1880.99	3.1399
130	7.16×10^{-4}	392.28	3.1331	7.50×10^{-4}	491.76	3.1352	6.96×10^{-4}	1787.38	3.1398

Reference:

1. Y. T. Cheng and G. W. Huber, *Acs Catal*, 2011, **1**, 611-628.
2. Y. T. Cheng, J. Jae, J. Shi, W. Fan and G. W. Huber, *Angewandte Chemie-International Edition*, 2012, **51**, 1387-1390.
3. J. R. Hufton and D. M. Ruthven, *Ind Eng Chem Res*, 1993, **32**, 2379-2386.
4. J. Crank, *The mathematics of diffusion*, Oxford University, London, 1956.